



2-2023

## The Role of Dynamic MRI in Hypovascular Hepatic Tumors

Abdulla nazir

*Department of Radiology, Faculty of Medicine for boys, Al-Azhar University, Cairo, Egypt*

Ahmed Seif

*Department of Radiology, Faculty of Medicine for boys, Al-Azhar University, Cairo, Egypt.*

Mohamed Soliman Ibrahim

*Department of Radiology, Faculty of Medicine for boys, Al-Azhar University, Cairo, Egypt.,  
ibrahimmohamedsoliman505@gmail.com*

Follow this and additional works at: <https://aimj.researchcommons.org/journal>



Part of the [Medical Sciences Commons](#), [Obstetrics and Gynecology Commons](#), and the [Surgery Commons](#)

### How to Cite This Article

nazir, Abdulla; Seif, Ahmed; and Ibrahim, Mohamed Soliman (2023) "The Role of Dynamic MRI in Hypovascular Hepatic Tumors," *Al-Azhar International Medical Journal*: Vol. 4: Iss. 2, Article 5.  
DOI: <https://doi.org/10.58675/2682-339X.1653>

This Original Article is brought to you for free and open access by Al-Azhar International Medical Journal. It has been accepted for inclusion in Al-Azhar International Medical Journal by an authorized editor of Al-Azhar International Medical Journal. For more information, please contact [dryasserhelmy@gmail.com](mailto:dryasserhelmy@gmail.com).

# The Role of Dynamic MRI in Hypo-vascular Hepatic Tumors

Abd Ellah Nazeer Yassin <sup>a,b</sup>, Ahmed Seif Al-Nasr Sediek <sup>a,b</sup>,  
Mohamed Soliman Ibrahim Elmatbouli <sup>a,b,\*</sup>

<sup>a</sup> Department of Radiology, Faculty of Medicine for Boys, Al-Azhar University, Cairo, Egypt

<sup>b</sup> Department of Radiology, Mansoura International Hospital, Mansoura, Egypt

## Abstract

**Background:** Despite new advances in liver imaging, it is still difficult to identify and classify hepatic focal lesions. It is particularly difficult in patients with cancer, where accurate tumor staging depends on the definition of the hepatic focal lesion for best treatment planning.

**Aim and objectives:** Was to evaluate the significance of dynamic magnetic resonance in identification and description of hypovascular hepatic tumor.

**Patients and methods:** Our current research study included 50 patients, comprising 34 men and 16 women, who had hepatic lesions that were detected using a variety of imaging modalities such as ultrasound, computed tomography scan, and dynamic and diffusion MRI.

**Results:** On noncontrast MRI, 26 lesions were detected in our 21 patients. Different signal intensities were displayed by these lesions on noncontrast MRI; we found that hypointensity in T1 is the commonest signal, whereas, hyperintensity was the commonest in T2 weighed image.

**Conclusion:** Reduced need for needless laparotomies for incurable illness may change patient treatment and result in considerable cost savings when liver metastases are detected as early as possible.

**Keywords:** Benign, Focal liver lesions, Malignant, MRI, Multiphases

## 1. Introduction

The liver is a prominent target for metastatic illness from practically any original malignant tumor and a main location of primary malignancies.<sup>1</sup> Furthermore, the adult population has a high frequency of benign liver lesions. Small hepatic hypovascular lesions are more often seen because of impressive advancements in diagnostic imaging of the liver.<sup>2</sup> Because both metastases and carcinoma are regarded as potentially lethal illnesses, it is crucial to distinguish between these lesions.<sup>3</sup>

The crucial component of the liver MRI procedure is gadolinium-enhanced T1-weighted images, which may increase liver lesion identification, anatomic portrayal, and characterization. T2-weighted imaging and MRI have both been recommended as

helpful supplements for the identification of liver metastases.<sup>4</sup> However, metastases were seen as a single homogeneous set of lesions in each of these trials.<sup>5</sup>

Compared with liver computed tomography (CT), MRI offers a number of benefits. Due to the high contrast provided by MRI, small differences in tissues with different histology may be seen.<sup>6</sup> Unlike CT scans, which can only be taken in the axial plane, MRIs may be acquired in any direction. Together, these MRI benefits provide superior detection and characterization abilities than CT does.<sup>7</sup>

Because treatment effectiveness and prognosis are higher in people with early-stage hepatocellular carcinoma (HCCs) than in those with advanced tumors, early diagnosis of HCC in at-risk patients is crucial. For bettering the early detection of HCCs,

Accepted 9 September 2022.

Available online 15 May 2023

\* Corresponding author at: Department of Radiology, Mansoura International Hospital, Mansoura, Egypt.  
E-mail address: [ibrahimmohamedsoliman505@gmail.com](mailto:ibrahimmohamedsoliman505@gmail.com) (M.S. Ibrahim Elmatbouli).

<https://doi.org/10.58675/2682-339X.1653>

2682-339X/© 2023 The author. Published by Al-Azhar University, Faculty of Medicine. This is an open access article under the CC BY-SA 4.0 license (<https://creativecommons.org/licenses/by-sa/4.0/>).

dynamic contrast-enhanced hepatic MRI has emerged as a crucial diagnostic technique.<sup>8</sup>

The most frequent benign tumor of the liver is hepatic cavernous hemangioma, and identification is often made based on distinctive imaging characteristics, such as peripheral globular centripetal and sustained elevation during dynamic imaging.<sup>9</sup>

The goal of the research was to evaluate the significance of dynamic magnetic resonance detection and characterization of hypovascular hepatic tumor.

## 2. Patients and methods

A total of 50 cases of hypovascular hepatic focal lesions were included in this investigation. The hospital run by Mansoura University served as the study's site. Over a period of 10 months, the patients received referrals from the Tropical Department to the Radiology Department (December 2020–September 2021). The patients' ages varied from 40 to 70 years (average 60 years); there were 14 female patients and 36 male patients.

### 2.1. Inclusion criteria

Patients known to have hypovascular hepatic focal lesion after diagnosed by different modalities such as ultrasound and CT triphasic were included.

### 2.2. Exclusion criteria

Contraindications to contrast agents, including those who have renal failure, those who are allergic to contrast agents, and those who should not undergo MRI due to claustrophobia, cardiac prostheses, or steel plates, were excluded.

All cases were subjected to the following: patients were planned for a thorough clinical evaluation, revision of the patient's laboratory tests such as kidney function tests (serum urea and serum creatinine), revision of the radiological tests previously completed for the patients, dynamic MRI with diffusion-weighted imaging (DWI), and histopathology to verify the lesion identified by dynamic MRI and DWI.

### 2.3. MRI

A 1.5-T MRI scanner (Philips Intera) with a phasedarray torso surface coil was used for the MRI.

### 2.4. Diffusion study

Before dynamic imaging, DWI was done utilizing a single-shot echo-planar sequence that was

respiratory triggered, fat-suppressed, and combined the two diffusion (motion-probing) gradients before and after the 180° pulse along the three directions of section selection, phase encoding, and frequency encoding. Data were acquired with an EPI readout by using three different b factors of 0, 500, and 1000 s/mm<sup>2</sup>. The acquisition time was shortened by using parallel imaging with generalized autocalibrating partially parallel acquisition and a two-fold acceleration. The following were the other factors: repetition time (TR) more than or equal to 1890 ms, echo time (TE) = 70 ms, number of excitations (NEX) = 3, matrix 124 × 120 with a field of view as small as possible, slice thickness 7–8 mm, slice gap 1–2 mm, and scan duration of 4–5 min.

### 2.5. Dynamic study

To prevent the effect of contrast agents on the apparent diffusion coefficient (ADC) value, a dynamic investigation was conducted following a diffusion assessment. After a bolus injection of 0.1 mmol/kg body weight of Gd-DTPA, which was flushed with 20 ml of sterile saline solution from the antecubital vein, a dynamic investigation was conducted. Manual administration of saline solution and contrast medium was done.<sup>10</sup> A triphasic approach to dynamic imaging employing the T1 THRIVE (examination of the isotropic volume in high resolution) technology was used. A dynamic series consisted of one pre contrast series, four subsequent postcontrast series, early arterial, late arterial, and portal venous phase imaging, with 18–21 s intervals (17–20 s) for image acquisition as per liver size, breath holding and 1 s for rebreathing for the beginning of each stage imaging, and 5 min of delayed stage imaging.<sup>11</sup> To reduce the chance of image misregistration, all patients were scanned near the conclusion of their treatment. The acquisition parameters were 3.3–4.5/1.4–1.9, the flip angle was 10°, the number of averaged signals was 1, the parallel imaging factor was 1.8, the matrix size was 172 × 135, the field of view was 300–400 mm, and the thickness of the slices was 2–3 mm.<sup>12</sup>

The following was determined from MRI: using a commercial Windows workstation (Philips), the size, border, signal features at T1, T2, and fat-saturated signal wavelengths, pattern of improvement in dynamic imaging, subtracted images, and signal intensity on diffusion images with ADC values and fusion images were all recorded as morphological characteristics of each lesion.<sup>13,14</sup>

## 2.6. Apparent diffusion coefficient measurement

Maps with pixel-based ADC were produced on the workstation.  $S = S_0 \times \exp(-b \times \text{ADC})$ , where  $S$  is the signal intensity after application of the diffusion gradient and  $S_0$  is the signal intensity at a  $b$  value of  $0 \text{ s/mm}^2$ , was used in a linear regression analysis to determine ADC. For the ADC computation, the three  $b$  values ( $0, 500, \text{ and } 1000 \text{ s/mm}^2$ ) were employed.<sup>15</sup> The center of the lesion on the DWI was established by the intersection point of two lines meeting at a right angle, which are a perpendicular line and a horizontal line from the top and left borders of the pictures, respectively. This allowed for exact placement of circular region of interest in tiny lesions. The same lines might be created on the matching ADC map using the line lengths as a guide. To assess the lesion's ADC, a circular region of interest was created around the central point using the lesion's size as a reference on the DWI. On diffusion pictures, a zone of focus was created over any sustained hyperintensity patches. If no high signal could be seen, the whole lesion was assessed.<sup>13</sup> The ADC was recorded three times, and the median of the three readings was calculated.

## 2.7. Statistical analysis

The analysis was conducted utilizing SPSS, version 15 software. The mean (as a measure of central tendency) and SD (as a measure of variability) were reported for quantitative variables. For qualitative factors, frequency and proportions were given. To evaluate differences in qualitative variables, the  $X^2$  test was applied. The region under the ROC curve, which stands for receiver operating characteristic, was created to illustrate prediction precision. Statistical significance was defined as a  $P$  value of 0.05 or below.

## 3. Results

A total of 50 patients, comprising 34 men and 16 women, who presented with hepatic lesions and were diagnosed using several imaging modalities, including ultrasound, CT scan, dynamic MRI, and diffusion MRI, were included in our current research.

The sex distribution in the studied cases shows a higher incidence of liver lesions in general among male patients (Fig. 1).

According to our MRI procedures, the final diagnosis of our cases was as follows: 17 (34%) of 50 cases were benign lesions, and 33 (66%) of 50 cases were malignant lesions. Hepatic metastases alone were seen in 34% (17 of 50). There was a high

prevalence of hemangioma among benign lesions (13 out of 17) 76.4%. Primary neoplasms detected by dynamic and DW MRI represented 39%, whereas secondaries and lymphoma detected by these advanced MRI techniques represented 29%. HCC had a high prevalence among malignant tumors [21 (42%) of 50]. The total number of malignant tumors detected by conventional MRI was 31 (62%), whereas the total number of malignant lesions detected by dynamic and DW MRI was 33 (66%) (Table 1).

Regarding benign lesion detection, there was no difference among dynamic MRI, DW MRI, and histopathology. Regarding malignant lesion detection, there was no substantial variation among dynamic MRI, DW MRI and histopathology. However, dynamic MRI failed in detection of three malignant lesions (Table 2).

Tables 3–5 show that on noncontrast MRI, 26 lesions were detected in our 21 patients. Different signal intensities were displayed by these lesions on noncontrast MRI. We found that hypointensity in T1 is the commonest signal, whereas hyperintensity is the commonest in T2 WI (Table 6).

There were no statistically significant differences found in the ADC values of various malignant lesions in the livers of cirrhotic and noncirrhotic individuals (Tables 7 and 8).

### Case no. 1

- (1) Clinical history: a 60-year-old male with a recent history of cancer colon underwent a ultrasound metastatic workup.
- (2) Conventional MRI: few small focal lesions at segments II, III, IV, and V; all showed bright signal in T2 (Fig. 2a).
- (3) Dynamic MRI: few small focal lesions at segments II, III, IV, and V; all showed no enhancement at any phase (Fig. 2b–d).
- (4) DWI: faint diffusion restriction (Fig. 2e).
- (5) Final diagnosis: the case of cancer colon shows hepatic focal lesion cystic metastasis.

### Case no. 2

- (1) Clinical history: a 65-year-old male patient with abdominal discomfort, dyspepsia, and jaundice.
- (2) Conventional MRI: right hepatic lobe segment VII well-developed focal lesion shows low signal in T2 with intrahepatic biliary radicles dilatations (Fig. 3a–c).
- (3) Dynamic MRI: right hepatic lobe segment VII focal lesion shows delayed peripheral contrast elevation with dilated intrahepatic biliary radicle dilatations (Fig. 3d–f).

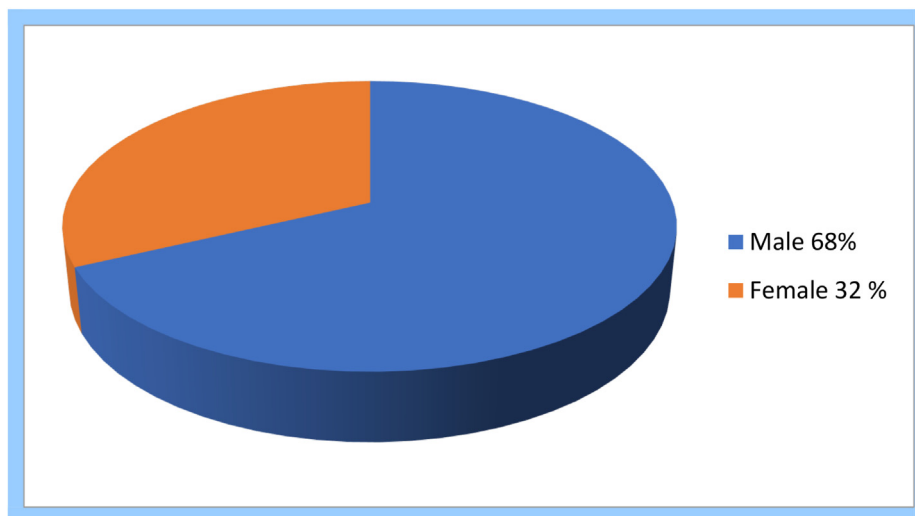


Fig. 1. Graph showed the incidence of sex distribution.

Table 1. Number and percentage of lesions detected by dynamic and diffusion weighed MRI.

Diagnosis	Cases no.	Lesions detected by dynamic MRI [n (%)]	Lesions detected by DW MRI [n (%)]
<b>Benign lesions</b>			
Hemangioma	11	11 (22)	11 (22)
Adenoma	4	4 (8)	4 (8)
Dysplastic nodules	2	2 (4)	2 (4)
Total benign lesions	17 (34)	17 (34)	17 (34)
<b>Malignant lesions</b>			
Primary neoplasms	16	16 (32)	16 (32)
Secondaries and lymphoma	17	14 (28)	17 (34)
Total malignant lesions	33 (66)	30 (60)	33 (66)
Total	50 (100)	47 (94)	50 (100)

DW, diffusion weighed.

- (4) DW MRI: evidence of diffusion restriction (bright signal in DWI and low in ADC map) (Fig. 3g and h).
- (5) Final diagnosis: right hepatic lobe segment VII cholangiocarcinoma.

#### 4. Discussion

The widespread use of dynamic enhancing studies is a reflection of the unusual vascular structure of the liver, which receives substantial venous blood flows from the gut and spleen through the hepatic portal system in addition to arterial blood from the systemic circulation via the hepatic arteries.<sup>16</sup>

The most popular multislice or volume spoiled gradient echo method used in multiphasic MRI scanning procedures enables high spatial resolution imaging of the whole area of interest within a single breath hold.<sup>17,18</sup>

According to our MRI procedures, the final diagnosis of our cases was as follows: 17 (34%) of 50 cases were benign lesions, and 33 (66%) of 50 cases were malignant lesions. Hepatic metastases alone represented 34% (17 of 50 cases). There was a high prevalence of hemangioma among benign lesions [13 (76.4%) of 17 cases]. Primary neoplasms detected by dynamic and DW MRI represented 39%, whereas

Table 2. Confirmation of detected lesions with histopathology.

Diagnosis	Histopathology [n (%)]	Lesions detected by dynamic MRI [n (%)]	Lesions detected by DW MRI [n (%)]	P value
Benign lesions	17 (34)	17 (34)	17 (34)	P1: 1 P2: 1
Malignant lesions	33 (66)	30 (60)	33 (66)	P1: 89 P2: 1

P1: histopathology and dynamic MRI.

P2: histopathology and diffusion weighed MRI.

Table 3. Morphological characters of 11 cases of hemangioma having 15 lesions in noncontrast MRI.

Pattern of enhancement	No.
Arterial phase	
Enhancing: peripheral nodular	8
Homogenous enhancement	2
Non enhancing	5
Portovenous phase	
Enhancing: peripheral nodular	5
Homogenous enhancement	2
Non enhancing	8
Delayed phase	
Enhancing: homogenous (complete fill in)	10
Incomplete filling	5

secondaries and lymphoma detected by these advanced MRI techniques represented 29%. HCC had a high prevalence among malignant tumors [21 (42%) of 50 cases]. The total number of malignant tumors detected by conventional MRI was 31 (62%), whereas the total number of malignant lesions detected by dynamic and DW MRI was 33 (66%).

Many researchers have categorized the findings from dynamic imaging of hepatic hemangioma into three patterns. Pattern I exhibits quick uniform increase (small capillary hemangioma (<1.5 cm)).<sup>19,20</sup>

Pattern II is characterized by a well-circumscribed hepatic mass with peripheral, nodular, and interrupted enhancement that may be larger than or equal to that of the blood pool and advances centripetally to uniform enhancement, the most typical of the three patterns. Pattern III is distinguished by prolonged central hypointensity and peripheral nodular increase with centripetal advancement (giant hemangioma >5 cm).

Median ADC value =  $1.77 + 0.11 \times 10^{-3} \text{ mm}^2/\text{s}$ .

Median ADC value =  $1.15 + 0.27 \times 10^{-3} \text{ mm}^2/\text{s}$ .

Table 4. Patterns of enhancement of 15 lesions in the 11 cases of hemangioma using dynamic MRI study.

Clinical symptoms and signs	Number of patients
Right hypochondrial pain	19
Dyspeptic symptoms (anorexia and vomiting)	17
Splenomegaly	16
Abdominal enlargement	18
Loss of weight	17
Positive HCV	13
Ascites	13
Hematemesis and melena	12
Jaundice	8
Hepatomegaly	7

Table 5. Different presentations in patients with hepatocellular carcinoma.

Morphological features	No.
Number	
Single	17
Multiple	4
Site	
Right lobe only	19
Left lobe only	4
Both lobes	6
Size	
<2 cm	10
2–5 cm	10
>5 cm	5
Exophytic extension	12
Tumor capsule	18

HCC is the highest prevalent primary malignant hepatic tumor, and on T1 WI, HCC is typically hypointense in relation to the liver; however, hyperintense lesions or pockets of hyperintensity within hypointense lesions may be detected. These hyperintense areas in the HCC are caused by intralesional bleeding and represent the existence of blood, copper, protein, or fat. Although well-differentiated tumors that are isointense in relation to the liver parenchyma may be observed, HCC is often hyperintense on T2 WI.<sup>21</sup>

Large HCC is more likely to exhibit signs of necrosis and often has a mosaic look made up of confluent tiny nodules with fibrous septa separating them and regions of necrosis. Such instances often present with tumor capsules, uneven borders, satellite nodules, and vascular extension.

Multiple associated radiological findings were found in our study, including radiological features of cirrhosis in 17 (75%) cases, splenomegaly in 13 (63%) cases, ascites in 10 (45%) cases, portal or IVC thrombosis in eight (30%) cases, and lastly, extra-hepatic mass in three (9%) cases.

Finding a tumor capsule might have therapeutic ramifications and is crucial for differential diagnosis. Because following surgical resection, encapsulated lesions have a better prognosis than unencapsulated lesions. Encapsulated lesions may be more susceptible to percutaneous ethanol ablation than unencapsulated lesions in individuals who are not candidates for surgery. The tumor capsule often

Table 6. Morphological features of 26 hepatocellular carcinoma lesions detected in 21 patients.

	Mean (SD)	Minimum–maximum
Cirrhosis positive	$0.73 \times 10^{-3} \text{ mm}^2/\text{s}$ (0.24)	0.40–1.17
Cirrhosis negative	$0.90 \times 10^{-3} \text{ mm}^2/\text{s}$ (0.25)	0.25–1.51
P value	<0.01 (statistically substantial)	

Table 7. Apparent diffusion coefficient of the liver parenchyma according to cirrhosis or not.

Morphological features	No.
No	
Single	13
Multiple	4
Location	
Right lobe only	13
Left lobe only	10
Both	3
Size	
<2 cm	14
2–5 cm	11
>5 cm	1

Table 8. Morphological features detected by conventional MRI in 21 patients having hepatic metastases in our study.

Lesion type	Mean ADC value (mm <sup>2</sup> /s)
Benign lesions	
Hemangioma	$1.77 + 0.11 \times 10^{-3}$
Adenoma	$1.15 + 0.27 \times 10^{-3}$
Malignant lesions	
HCC	$0.81 + 0.15 \times 10^{-3}$
Metastasis	$0.78 + 0.16 \times 10^{-3}$
Cholangiocarcinoma mets	1.131 135.0

ADC, apparent diffusion coefficient; HCC, hepatocellular carcinoma.

exhibits low signal strength on unenhanced T1 and T2 WI; however, a capsule thicker than 4 mm may exhibit an exterior layer with significant signal intensity on T2 WI. However, the capsule is often only

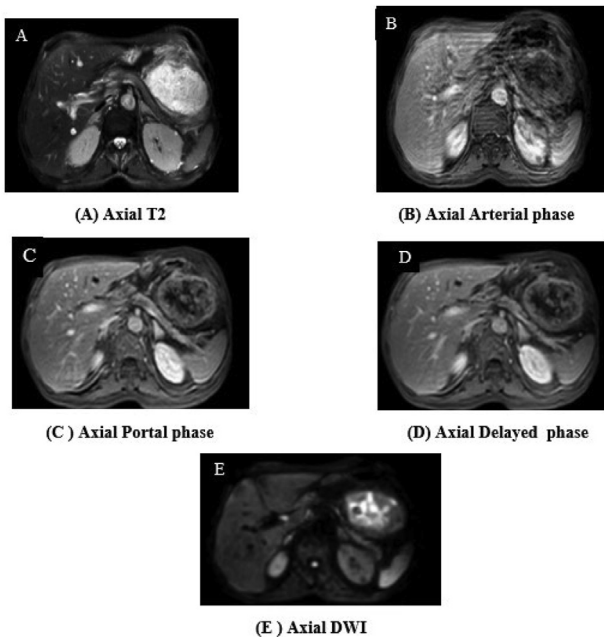


Fig. 2. (a) Axial T2, (b) axial arterial phase, (c) axial portal phase, (d) axial delayed phase, and (e) axial DWI.

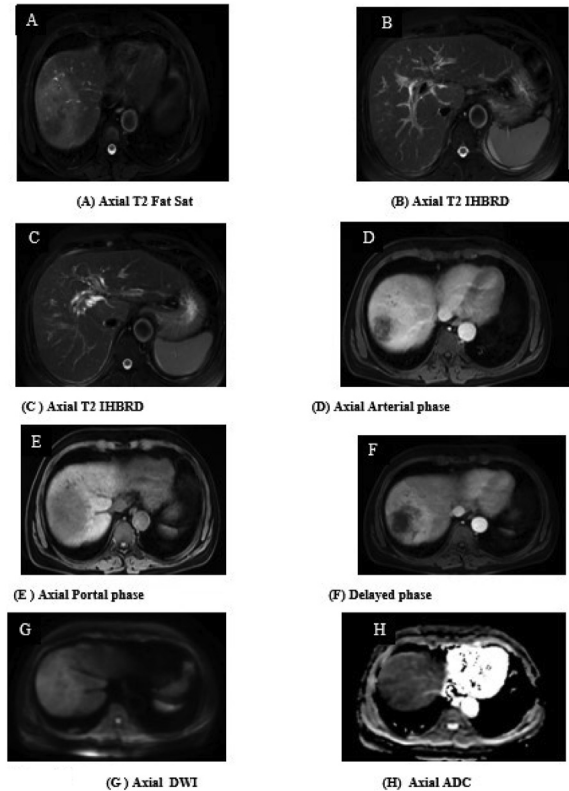


Fig. 3. (a) Axial T2 fat sat, (b) axial T2 IHRD, (c) axial T2 IHRD, (d) axial arterial phase, (e) axial portal phase, (f) delayed phase, (g) axial DWI, and (h) axial ADC. ADC, apparent diffusion coefficient; DWI, diffusion-weighted imaging.

seen on post-Gd T1 WI during the venous or delayed phases.<sup>8</sup>

Contrary to hypervascular metastases, which enhance sooner, are best visible on arterial phase imaging, and exhibit washout on delayed pictures, hypovascular metastases show lower enhancement compared with normal liver and are most noticeable on portovenous phase images.<sup>21</sup>

#### 4.1. Conclusion

Imaging characteristics comparable to those of HCC and ICC may be seen in a number of benign liver diseases. It is important to recognize the distinctive MRI features of different benign tumors to prevent a false-positive diagnosis of HCC or ICC and the ensuing need for intrusive treatment. Differentiating these lesions from HCC and ICC requires thorough imaging, as well as a study of clinical and histological data.

#### Conflict of interest

Authors declare that there is no conflict of interest, no financial issues to be declared.

## References

- Oien KA. Pathologic evaluation of unknown primary cancer. *Semin Oncol.* 2009;36:8–37.
- Qian H, Li S, Ji M, Lin G. MRI characteristics for the differential diagnosis of benign and malignant small solitary hypovascular hepatic nodules. *Eur J Gastroenterol Hepatol.* 2016;28:749–756.
- Lambert AW, Pattabiraman DR, Weinberg RA. Emerging biological principles of metastasis. *Cell.* 2017;168:670–691.
- Albiin N. MRI of focal liver lesions. *Curr Med Imag Rev.* 2012;8:107–116.
- Halama N, Spille A, Lerchl T, Brand K, Herpel E, Welte S, et al. Hepatic metastases of colorectal cancer are rather homogeneous but differ from primary lesions in terms of immune cell infiltration. *Oncolmmunology.* 2013;2, e24116.
- Choi JY, Lee JM, Sirlin CB. CT and MR imaging diagnosis and staging of hepatocellular carcinoma: part II. Extracellular agents, hepatobiliary agents, and ancillary imaging features. *Radiology.* 2014;273:30–50.
- Histed SN, Lindenberg ML, Mena E, Turkbey B, Choyke PL, Kurdziel KA. Review of functional/anatomical imaging in oncology. *Nucl Med Commun.* 2012;33:349–361.
- Bruix J, Reig M, Sherman M. Evidence-based diagnosis, staging, and treatment of patients with hepatocellular carcinoma. *Gastroenterology.* 2016;150:835–853.
- Bajenaru N, Balaban V, Săvulescu F, Campeanu I, Patrascu T. Hepatic hemangioma – review. *J Med Life.* 2015;8:4–11.
- Madbouly M, Hamzawy D, Hassan M, Desouky S, Hamed El-Ghawaby MD, Ahmed Abdelsamie MD. Role of diffusion-weighted magnetic resonance imaging in detecting and characterizing benign and malignant liver tumors in adults. *Med J Cairo Univ.* 2021;89:229–236.
- Osama RM, Abdelmaksoud AH, El Tatawy SA, Nabeel MM, Metwally LI. Role of dynamic contrast-enhanced and diffusion weighted MRI in evaluation of necrosis of hepatocellular carcinoma after chemoembolization. *Egypt J Radiol Nucl Med.* 2013;44:737–746.
- Guirguis MS, Moftah SG, Abdelkhalek YI, Elshawaf WF, Mohammed AM. Role of dynamic contrast-enhanced and diffusion weighted mri in evaluation of response of hepatocellular carcinoma after chemoembolization. *Ain Shams Med J.* 2019;70:759–769.
- Yu J-S, Kim JH, Chung J-J, Kim KW. Added value of diffusion-weighted imaging in the MRI assessment of perilesional tumor recurrence after chemoembolization of hepatocellular carcinomas. *J Magn Reson Imag.* 2009;30:153–160.
- Zhang L, Hu J, Guys N, et al. Diffusion-weighted imaging in relation to morphology on dynamic contrast enhancement MRI: the diagnostic value of characterizing non-puerperal mastitis. *Eur Radiol.* 2018;28:992–999.
- Zenat A, Mona AAE, Abdel Aziz MD, Mohamed M. Role of apparent diffusion coefficient (ADC) mapping in assessment of therapeutic response of hepatocellular carcinoma post trans-catheter arterial chemoembolization. *Med J Cairo Univ.* 2021;89:1533–1541.
- Eipel C, Abshagen K, Vollmar B. Regulation of hepatic blood flow: the hepatic arterial buffer response revisited. *World J Gastroenterol.* 2010;16:6046–6057.
- Wáng YXJ, Wang X, Wu P, et al. Topics on quantitative liver magnetic resonance imaging. *Quant Imag Med Surg.* 2019;9:1840–1890.
- Kim Y-C. Advanced methods in dynamic contrast enhanced arterial phase imaging of the liver. *Invest Magn Reson Imag.* 2019;23:1.
- Heiken JP. Distinguishing benign from malignant liver tumours. *Cancer Imag.* 2007;7:1–14.
- Zhu K, Wang W, Luo R, et al. Newly detected liver nodules with a history of colorectal cancer: are they metastatic? Review of 2,632 cases in a single center. *Ann Transl Med.* 2021;9:1079.
- Cho ES, Choi JY. MRI features of hepatocellular carcinoma related to biologic behavior. *Korean J Radiol.* 2015;16:449–464.